# Theoretical prediction for the $(AlN)_{12}$ fullerene-like cage-based nanomaterials



2007 J. Phys.: Condens. Matter 19 346228

(http://iopscience.iop.org/0953-8984/19/34/346228)

IOP PUBLISHING JOURNAL OF PHYSICS: CONDENSED MATTER

J. Phys.: Condens. Matter **19** (2007) 346228 (8pp) doi:10.1088/0953-8984/19/34/346228

# Theoretical prediction for the $(AlN)_{12}$ fullerene-like cage-based nanomaterials

**Jiling Li[1], Yueyuan Xia[1], Mingwen Zhao[1], Xiangdong Liu[1], Chen Song[1], Lijuan Li[1], Feng Li[2] and Boda Huang[3]**

[1] School of Physics and Microelectronics, Shandong University, Jinan, Shandong 250100, People's Republic of China
[2] Department of Physics, Taishan University, Taian, Shandong 271021, People's Republic of China
[3] School of Information Science and Engineering, Shandong University, Jinan 250100, People's Republic of China

E-mail: yyxia@sdu.edu.cn

Received 22 May 2007, in final form 6 July 2007
Published 26 July 2007
Online at stacks.iop.org/JPhysCM/19/346228

**Abstract**

We have performed *ab initio* calculations on the stability and structural and electronic properties of the fullerene-like cage $(AlN)_n$ ($n = 12$) and the polymerized dimers and nanowires obtained from it. We found that the $(AlN)_{12}$–$(AlN)_{12}$ dimers and aluminum nitride $(AlN)_{12}$-based nanowires polymerized from the $(AlN)_{12}$ cage are more stable than $(AlN)_{12}$. The optimized configurations of the nanowires are especially regular and exhibit an interesting dumbbell-shaped chain structure. We also calculated the electronic structures of all the constructed nanostructures. The two novel $(AlN)_{12}$-based aluminum nitride nanowires have band gaps of 2.844 and 3.085 eV, respectively, implying that they are both wide-gap semiconductors and may be promising candidates for nanotechnology.

(Some figures in this article are in colour only in the electronic version)

## 1. Introduction

In recent years, more and more experimental and theoretical efforts have been devoted to the study of possible fullerene-like structures and nanotubes constructed of other elements, rather than carbon, for their specific physical and chemical properties [1–6]. In particular, III–V fullerene-like cages and tubular structures have been theoretically predicted [7–9] and experimentally synthesized [10–13]. Generally, III–V compounds, especially the group III nitrides, are found to be an important source of nanoscale materials for their direct band gaps affording optical and electrooptical properties that are of considerable importance to science and technology. Among these, aluminum nitride semiconductor nanostructures are especially promising materials and have attracted considerable attention due to their large band gap, low

electron affinity and excellent physical and chemical properties, e.g. high thermal conductivity, low thermal expansion coefficient and chemical inertness. Recently, theoretical investigations addressing the stability of aluminum nitride nanostructures based on *ab initio* calculations were reported [9]. The structures and stability of fullerene-like cages of $(AlN)_n$ ($n = 2$–41) were studied and it was suggested that the fullerene-like cage $(AlN)_{12}$ is energetically the most stable cluster in this family and would thus be an ideal inorganic fullerene-like cage. In the theoretical studies on the $(BN)_n$ [1] and $(SiC)_n$ [2] clusters, the fullerene-like cages $(BN)_{12}$ and $(SiC)_{12}$ were also predicted to be the most stable ones. These facts indicate that the fullerene-like cage $(XY)_n$ may be a magic cluster and have inherent special stability when $n$ is equal to 12. On the other hand, since the first report on the polymerization of the $C_{60}$ fullerene using photoirradiation [14], the experimental Raman [15] or IR [16, 17] spectra and the related theoretical calculations [18–20] have provided significant information on the polymerization of $C_{60}$ fullerene. Simultaneously, various techniques, such as high-pressure and high-temperature processing, alkali-metal doping, mechanochemical reaction and electron-beam irradiation, were used to prepare polymerized $C_{60}$ materials. However, to our knowledge, studies of the polymerization of binary fullerene-like cages consisting of elements other than carbon have not been reported so far. Considering the promising applications of the aluminum nitride nanomaterials, the experimental and theoretical exploration of the polymerization of $(AlN)_n$ fullerene-like clusters is an interesting subject. In this contribution, we performed an *ab initio* study of the structural stabilities and the electronic properties of the fullerene-like cage $(AlN)_{12}$, the $(AlN)_{12}$–$(AlN)_{12}$ dimers and the $(AlN)_{12}$-based aluminum nitride nanowires polymerized from the $(AlN)_{12}$ clusters. We focus our attention on different conformations of the $(AlN)_{12}$-based materials, including two $(AlN)_{12}$–$(AlN)_{12}$ dimers and two $(AlN)_{12}$-based one-dimensional chain nanowires. We hope that our theoretical study of the fullerene-like cage $(AlN)_{12}$ and the $(AlN)_{12}$-based nanostructures will provide a useful guide for the experimental search for synthesis methods for these novel aluminum nitride nanomaterials.

## 2. Theoretical approaches and computations

We performed *ab initio* calculations using the SIESTA code [21–23], which is based on the standard Kohn–Sham self-consistent density functional theory (DFT). A flexible linear combination of numerical atomic-orbital basis sets was used for the description of valance electrons and norm-conserving nonlocal pseudopotentials were adopted for the atomic cores. The pseudopotentials were constructed using the Trouiller–Martins scheme [24] to describe the interaction of valance electrons with the atomic cores. The nonlocal components of the pseudopotential were expressed in the fully separable form of Kleiman and Bylander [25, 26]. The Perdew–Burkle–Ernzerhof (PBE) form of generalized gradient approximation (GGA) corrections was adopted for the exchange–correction potential [27]. The atomic orbital basis set employed throughout was a double-$\zeta$ plus polarization (DZP) function. The numerical integrals were performed and projected on a real space grid with an equivalent cutoff of 120 Ryd to calculate the self-consistent Hamiltonian matrix elements. The fullerene-like cage $(AlN)_{12}$ and all the $(AlN)_{12}$-based nanostructures obtained from $(AlN)_{12}$ were studied using the same converging conditions. For the two $(AlN)_{12}$-based aluminum nitride 1D nanowires under study, we adopt a supercell with a periodic boundary condition in the direction parallel to the tube axis (the $z$ direction in figure 1(d)), and with a lateral vacuum region larger than 20 Å to avoid image interactions. The supercell of the $(AlN)_{12}$-based aluminum nitride nanowires contains one $(AlN)_{12}$–$(AlN)_{12}$ dimer component as a translational unit. To determine the equilibrium configurations of these $(AlN)_{12}$-based nanomaterials, we relaxed all the atomic coordinates involved by using a conjugate gradient (CG) algorithm, until the maximum atomic force was

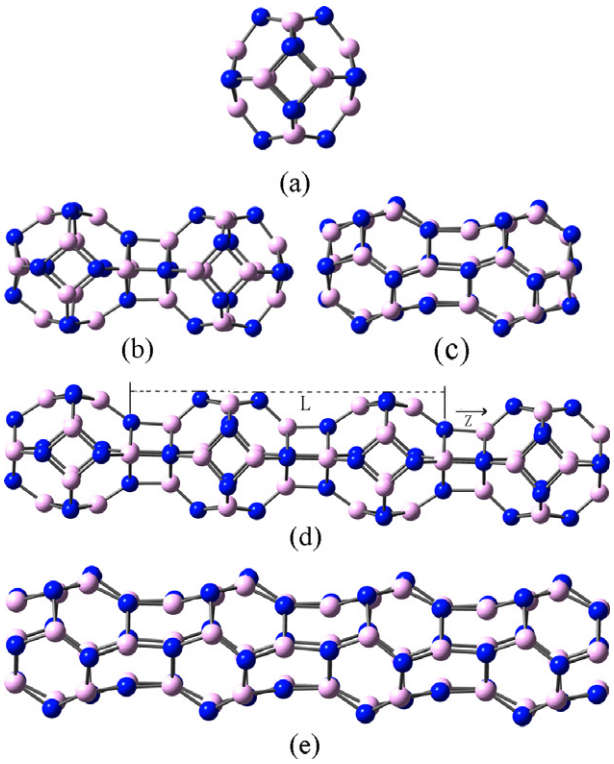


**Figure 1.** The optimized configurations of the fullerene-like cage $(AlN)_{12}$ and $(AlN)_{12}$-based aluminum nitride nanostructures: (a) fullerene-like cage $(AlN)_{12}$, (b) $(AlN)_{12}$–$(AlN)_{12}$ dimer (I), (c) $(AlN)_{12}$–$(AlN)_{12}$ dimer (II), (d) $(AlN)_{12}$-based nanowire (I) and (e) $(AlN)_{12}$-based nanowire (II) obtained from coalescing of $(AlN)_{12}$–$(AlN)_{12}$ units. The translational periodicity of the two kinds of nanowires shown in (d) and (e) is $L = 14.83$ Å and 13.22 Å, respectively. (The black (blue) color is for N atoms and the gray (pink) color for Al atoms.)

less than 0.02 eV/Å. The convergence of the total energies of the nanostructures under study was checked using different $k$ sampling in the Brillouin zone, $1 \times 1 \times 8$ and $1 \times 1 \times 16$, according to the Monkhorst–Pack scheme [28]. The differences in total energies between the results are less than 0.07 meV/atom. Binding energies were calculated according to the expression

$$E_b = (E - mE_{Al} - nE_N)/(m + n) \quad (1)$$

where $E$ is the total energy of the $(AlN)_{12}$-based aluminum nitride nanostructure, $m$ and $n$ are the number of the Al and N atoms involved, respectively, and $E_{Al}$ and $E_N$ are the energies of an isolated Al and N atom, respectively; they are calculated using the same basis set and $k$-point sampling as those used for the aluminum nitride nanostructures under study.

## 3. Results and discussions

We first determined the equilibrium configurations of the fullerene-like cage $(AlN)_{12}$ and the $(AlN)_{12}$-based nanomaterials as shown in figure 1. Our calculations indicate that the fullerene-like cage $(AlN)_{12}$ and the $(AlN)_{12}$-based nanomaterials under study show structural stability, since all of them keep the basic structural feature of the intact $(AlN)_{12}$. First, we analyzed the possible structure of the fullerene-like cage $(AlN)_{12}$. Previous theoretical study of $(AlN)_n$

clusters and nanotubes indicated that aluminum nitride nanomaterials having the Al atoms and N atoms allocated alternatively are more stable. The initial structure of the $(AlN)_{12}$ cage can be constructed based on the ad hoc rule of alternative distribution of Al atoms and N atoms, and on the method used for constructing $(AlN)_n$ clusters [9], following the conclusions that the polyhedrons of fullerene-like clusters having four-numbered rings (4NRs) and six-numbered rings (6NRs) on the cage faces show higher stability [29]. As deduced from the Euler polytope [30], for the $(XY)_n$ fullerene-like cage consisting of 4NRs and 6NRs, the number of 4NRs is always equal to 6, while the number of 6NRs is $n - 4$. Besides, the stability of the constructed cages depends on the separation of the faces of the 4NRs, the larger the separation, the more stable the system, and the cage molecule with the maximal separation of 4NR faces should be the most stable one, in line with the pentagon rule in fullerene chemistry [31]. Following the rules mentioned above, we constructed the initial fullerene-like cage $(AlN)_{12}$ and optimized the configuration using the *ab initio* computation code SIESTA. The optimized configuration of the $(AlN)_{12}$, which has six 4NRs and eight 6NRs, is found to be $T_h$ symmetry, as shown in figure 1(a). The Al–N bond lengths between the aluminum atoms and nitrogen atoms in the 4NRs have a unique length of 1.89 Å, which is exactly the same as that of bulk AlN(zinc blende) of 1.89 Å and longer than those in the 6NRs, 1.82 Å. The bond angles of Al–N–Al and N–Al–N in the 6NRs are 109.5° and 127.9°, respectively, while in the 4NRs they are respectively 83.6° and 94.4°. The optimized configuration of the fullerene-like cage $(AlN)_{12}$ we obtained using the SIESTA code is in good agreement with the results of [9], where they drew the conclusion that $(AlN)_{12}$ is the most stable one and should be an ideal candidate for a fullerene-like cage.

In the following, we will focus our attention on the polymerization of the fullerene-like cage $(AlN)_{12}$. The optimized configurations of the $(AlN)_{12}$ derivatives are shown in figures 1(b)–(e). The two $(AlN)_{12}$–$(AlN)_{12}$ dimers, shown in figures 1(b) and (c), were just obtained from the $(AlN)_{12}$ cages by coalescing two 4NRs of two $(AlN)_{12}$ clusters and two 6NRs of two $(AlN)_{12}$ clusters, respectively, followed by global structural optimization processes. As shown in figures 1(b) and (c), both of the optimized $(AlN)_{12}$–$(AlN)_{12}$ dimer structures have very good axial symmetry features. Therefore, the $(AlN)_{12}$-based aluminum nitride nanowires can be formed by translational symmetry arrangement. The segments of the structurally optimized $(AlN)_{12}$-based aluminum nitride nanowires obtained are shown in figures 1(d) and (e). To study the stability of the $(AlN)_{12}$-based aluminum nitride dimers and nanowires, we calculated their binding energies in accordance with equation (1). The calculated binding energies of the $(AlN)_{12}$–$(AlN)_{12}$ dimer (I) (figure 1(b)) and dimer (II) (figure 1(c)), are about 139 and 194 meV/atom, respectively, higher than that of the fullerene-like cage $(AlN)_{12}$ shown in figure 1(a). Therefore, these $(AlN)_{12}$–$(AlN)_{12}$ dimers are more stable than the fullerene-like cage $(AlN)_{12}$. The $(AlN)_{12}$–$(AlN)_{12}$ dimer (II) is more stable than the $(AlN)_{12}$–$(AlN)_{12}$ dimer (I). The calculated binding energies of the $(AlN)_{12}$-based nanowire (I) (figure 1(d)) and $(AlN)_{12}$-based nanowire (II) (figure 1(e)) are respectively 278 and 389 meV/atom higher than that of the $(AlN)_{12}$ cage. In terms of favorable energy order, among all these structures under study the $(AlN)_{12}$-based AlN nanowire (II) is the most stable, followed by the $(AlN)_{12}$-based AlN nanowire (I), the $(AlN)_{12}$–$(AlN)_{12}$ dimer (II), the $(AlN)_{12}$–$(AlN)_{12}$ dimer (I) and finally the $(AlN)_{12}$ cage. This demonstrates obviously that the stabilities of the $(AlN)_{12}$-based nanomaterials show an increasing trend with increasing size of the cluster by the polymerization of the $(AlN)_{12}$. Therefore, it is reasonable to deduce that if the fullerene-like cage $(AlN)_{12}$ could be synthesized experimentally, it would be easier to synthesize the $(AlN)_{12}$-based aluminum nitride nanowires. This may be a guide for the experimental scientists in their search for novel $(AlN)_{12}$-based nanowires as a new kind of aluminum nitride nanomaterial.

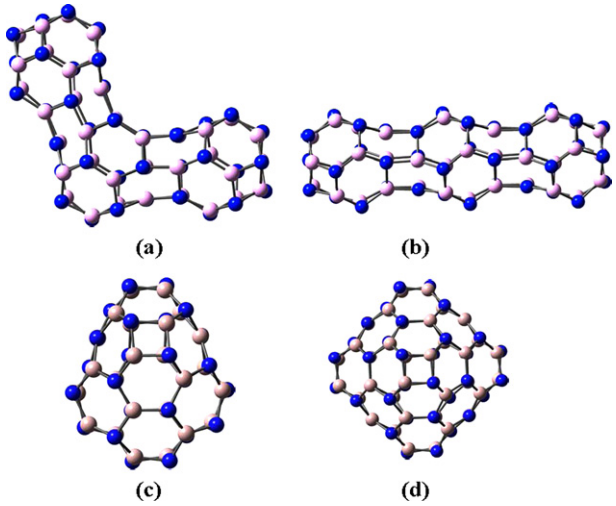


**Figure 2.** The optimized configurations of (a) $(AlN)_{12}$-based trimer (I), (b) $(AlN)_{12}$-based trimer (II), (c) $(AlN)_{24}$ spheroid and (d) $(AlN)_{36}$ spheroid. (The black (blue) color is for N atoms and the gray (pink) color for Al atoms.)

From the optimized configurations of both the $(AlN)_{12}$-based aluminum nitride nanowires, shown in figures 1(d) and (e), it is clear that the polymeric nanostructures show a unique one-dimensional chain nanostructure. The Al–N bonds forming the 'necks' joining the unit cells have the same length of 1.93 Å, which is just the same as the bond length of the bulk AlN (zinc blende) we calculated. Other Al–N bond lengths of both aluminum nitride nanowires have diverse values of 1.81, 1.82, 1.87 and 1.89 Å. The special dumbbell-shaped chain structure and the binary nanomaterial feature make these aluminum nitride nanowires particularly attractive for finding novel applications.

To examine whether nanostructures other than those shown in figure 1 would be formed by polymerizing the $(AlN)_{12}$ clusters at different reaction sites, we made a 6NR of a $(AlN)_{12}$ cage coalesce with a 6NR of the $(AlN)_{12}$–$(AlN)_{12}$ dimer (II) to form a bent trimer (I) upon structural optimization, as shown in figure 2(a). In comparison with the trimer (II) (figure 2(b)) formed by joining the $(AlN)_{12}$ cage with the $(AlN)_{12}$–$(AlN)_{12}$ dimer (II) in the axial direction, the trimer (I) has binding energy about 2.3 meV/atom lower than that of trimer (II). Since the binding energy of the trimer (II) is a bit higher than that of the bent structure of the trimer (I), the formation of the chain structure of the $(AlN)_{12}$-based nanowire (II) is energetically a bit more favorable than a branched nanowire. We also constructed and optimized the structures of an $(AlN)_{24}$ spheroid and an $(AlN)_{36}$ spheroid following the rules based on $(AlN)_{12}$. The optimized configurations are shown in figures 2(c) and (d), respectively. The binding energy of the $(AlN)_{12}$–$(AlN)_{12}$ dimer (II) is about 13 meV/atom higher than that of the $(AlN)_{24}$ spheroid, while the binding energy of the trimer (II) is about 9 meV/atom lower than that of the $(AlN)_{36}$ spheroid. The small differences between the binding energies indicate that complicated aluminum nitride nanostructures may coexist in the products during the synthesis process.

To gain further understanding of the properties of the fullerene-like cage $(AlN)_{12}$ and the $(AlN)_{12}$-based nanomaterials considered above, we have calculated the electronic structures of all the configurations shown in figure 1. The energy gaps between the HOMO and LUMO for the nanostructures under study are listed in table 1. The HOMO–LUMO gaps of the

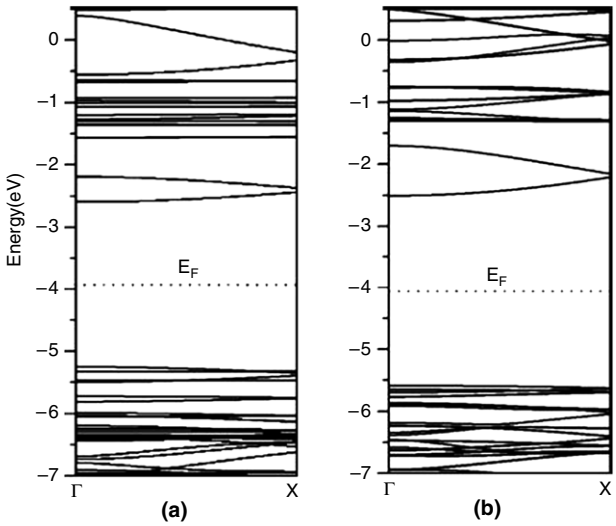


**Figure 3.** The energy band structures of (a) $(AlN)_{12}$-based aluminum nitride nanowire (I), and (b) $(AlN)_{12}$-based aluminum nitride nanowire (II).

**Table 1.** The energy gaps ($\Delta E$) between the HUMO and LUMO of the fullerene-like cage $(AlN)_{12}$, $(AlN)_{24}$, $(AlN)_{36}$ and the $(AlN)_{12}$-based nanostructures under study.

| Material | $\Delta E = E_{\mathrm{HOMO}} - E_{\mathrm{LUMO}}$ (eV) |
|---|---|
| $(AlN)_{12}$ | 2.766 |
| $(AlN)_{12}$–$(AlN)_{12}$ dimer (I) | 2.713 |
| $(AlN)_{12}$–$(AlN)_{12}$ dimer (II) | 2.884 |
| $(AlN)_{12}$-based nanowire (I) | 2.662 |
| $(AlN)_{12}$-based nanowire (II) | 3.085 |
| $(AlN)_{36}$ trimer (I) | 2.913 |
| $(AlN)_{36}$ trimer (II) | 2.726 |
| $(AlN)_{24}$ spheroid | 2.481 |
| $(AlN)_{36}$ spheroid | 2.726 |

$(AlN)_{12}$–$(AlN)_{12}$ dimer (I) and $(AlN)_{12}$-based nanowire (I) are both smaller than that of the isolated $(AlN)_{12}$ cluster, while those of the $(AlN)_{12}$–$(AlN)_{12}$ dimer (II) and the $(AlN)_{12}$-based nanowire (II) have larger energy gaps than that of the $(AlN)_{12}$ cluster.

We also calculated the electronic energy band structures of the $(AlN)_{12}$-based aluminum nitride nanowires. The energy bands near the Fermi surface are shown in figure 3. Here, we take the mid-gap energies as valid Fermi levels and denote them by the dashed lines. The two band structures clearly show finite band gaps, with widths of 2.662 eV for the $(AlN)_{12}$-based aluminum nitride nanowire (I) (figure 3(a)) and 3.085 eV for the $(AlN)_{12}$-based aluminum nitride nanowire (II) (figure 3(b)). Comparing the band-gap widths of the structures listed in table 1, it is clear that the formation of the tubular linkage structures does not cause remarkable change in band-gap width. Both the $(AlN)_{12}$-based aluminum nitride nanowires have semiconducting electrical properties with direct energy gaps. The feature of wide and direct energy gaps is particularly attractive for application in optoelectronic devices working in the short-wavelength region.

For a better understanding of the band structures of the $(AlN)_{12}$-based aluminum nitride nanowire (I) and $(AlN)_{12}$-based aluminum nitride nanowire (II), we present the density of states

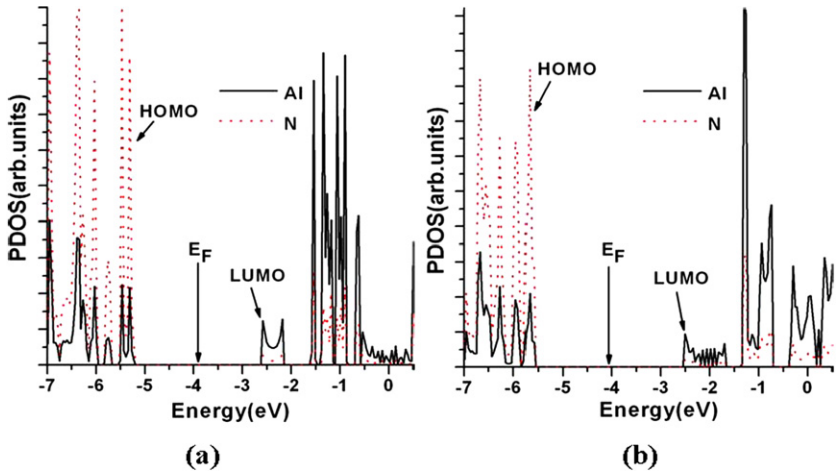


**Figure 4.** PDOS of the $(AlN)_{12}$-based aluminum nitride nanowires projected to Al atoms (solid (black) line) and N atoms (dotted (red) line), respectively: (a) $(AlN)_{12}$-based aluminum nitride nanowire (I) and (b) $(AlN)_{12}$-based aluminum nitride nanowire (II). The Fermi levels are denoted by the arrows in this figure.

projected to different atoms (PDOS) of them in figures 4(a) and (b), respectively. The Gaussian widths employed in plotting both the PDOS are 0.02 eV. The mid-gap energies are also taken as the valid Fermi levels and denoted by the arrows, as shown in figure 4. For both of the $(AlN)_{12}$-based nanowires, the electron states near the top of the valence band are mainly contributed by the nitrogen atoms while those near the bottom of the conduction band are mainly contributed by the aluminum atoms. This is mainly due to the charge transfer from the Al atoms to the N atoms. The energy band structures of these $(AlN)_{12}$-based aluminum nitride nanowires are similar to the aluminum nitride nanotubes (AlNNTs) [32]. It is worth further study to find the path of synthesis of these novel and promising materials as a new kind of aluminum nitride nanomaterial.

## 4. Conclusions

Our calculations show that the stable fullerene-like cage $(AlN)_{12}$ can form a new family of aluminum nitride nanostructures, including $(AlN)_{12}$-based dimers and nanowires, which are energetically more stable than the $(AlN)_{12}$ cluster from the viewpoint of binding energy. The fully optimized structures of the two $(AlN)_{12}$-based nanowires are especially regular and exhibit interesting stable dumbbell-shaped chain structures with translational periodicities along the directions of their axes. The HOMO–LUMO gaps of these configurations of $(AlN)_{12}$-based materials are not recognized to have a remarkable difference in energy-gap width from the $(AlN)_{12}$ cluster. The $(AlN)_{12}$-based nanowire (I) and (II) have direct band gap of 2.662 eV and 3.085 eV, respectively. We hope that this finding could motivate further studies on the $(AlN)_{12}$-based materials, for instance on the synthesis methods and applications and functionalization of this novel material family.

## Acknowledgments

This work is supported by the National Natural Science foundation of China under grant nos 10675075, 50402017 and 10604039, and supported by the National Basic Research Program

of China under grant no. 2005CB623602. M Zhao thanks the Program for New Century Excellent Talents in University of China for support. XL thanks the Outstanding Youth Scientist Research Foundation of Shandong Province, and the Foundation of Education Ministry of China for funding support under grant nos 2006BS04012 and 20050422006, and BH thanks the Excellent Middle-Aged and Young Scientist Award Foundation of Shandong Province for funding support under grant no. 2004BS5007.

## References

[1] Strout D L 2000 *J. Phys. Chem.* A **104** 3364
[2] Wang R X, Zhang D J and Liu C B 2005 *Chem. Phys. Lett.* **411** 333
[3] Bertolus M, Finocchi F and Millié P 2004 *J. Chem. Phys.* **120** 9
[4] Golberg D, Bando Y, Stéphan O and Kurashima K 1998 *Appl. Phys. Lett.* **73** 17
[5] Stafström S, Hultman L and Hellgren N 2001 *Chem. Phys. Lett.* **340** 227
[6] Fu C-C, Weissmann M, Machado M and Ordejón P 2001 *Phys. Rev.* B **63** 085411
[7] Lee S M, Lee Y H, Hwang Y G, Elsner J, Porezag D and Frauenheim T 1999 *Phys. Rev.* B **60** 7788
[8] Seifert G and Hernandez E 2000 *Chem. Phys. Lett.* **318** 355
[9] Wu H S, Zhang F Q, Xu X H, Zhang C J and Jiao H 2003 *J. Phys. Chem.* A **107** 204
[10] Hacohen Y R, Grunbaum E, Tenne R and Hutchison J L 1998 *Nature* **395** 336
[11] Feldman Y, Wasserman E, Srolovitz D J and Tenne R 1995 *Science* **267** 222
[12] Balasubramanian C, Belluci S, Castrucci P, Crescenzi M D and Bhoraskar S V 2004 *Chem. Phys. Lett.* **383** 188
[13] Bourgeois L, Bando Y, Han W Q and Sato T 2000 *Phys. Rev.* B **61** 7686
[14] Rao A M *et al* 1993 *Science* **259** 955
[15] Onoe J, Hashi Y, Esfarjani K, Hara T, Kawazoe Y and Takeuchi K 1999 *Chem. Phys. Lett.* **315** 19
[16] Bandow S, Takizawa M, Hirahara H, Yudasaka M and Iijima S 2001 *Chem. Phys. Lett.* **337** 48
[17] Onoe J, Nakayama T, Aono M and Hara T 2003 *Appl. Phys. Lett.* **82** 595
[18] Wang G, Li Y X and Huang Y H 2005 *J. Phys. Chem.* B **109** 10957
[19] Tsukamoto S and Nakayama T 2005 *J. Chem. Phys.* **122** 074702
[20] Beu T A, Onoe J and Hida A 2005 *Phys. Rev.* B **72** 155416
[21] Ordejón P, Artacho E and Soler J M 1996 *Phys. Rev.* B **53** R10441
[22] Sánchez-Portal D, Ordejon P, Artacho E and Soler J M 1997 *Int. J. Quantum Chem.* **65** 453
[23] Soler J M, Artacho E, Gale J D, Garcia A, Junquera J, Ordejón P and Sánchez-Portal D 2002 *J. Phys.: Condens. Matter* **14** 2745 and references therein
[24] Troullier N and Martins J L 1991 *Phys. Rev.* B. **43** 1993
[25] Kleinman L and Bylander D M 1982 *Phys. Rev. Lett.* **48** 1425
[26] Bylander D M and Kleinman L 1990 *Phys. Rev.* B **41** 907
[27] Perdew J P, Burke K and Ernzerhof M 1996 *Phys. Rev. Lett.* **77** 3865
[28] Monkhorst H J and Pack J D 1976 *Phys. Rev.* B. **13** 5188
[29] Zurek E, Woo T K, Firman T K and Ziegler T 2001 *Inorg. Chem.* **40** 361
[30] Coxeter H S M 1961 *Introduction to Geometry* (New York: Wiley)
See also Cerari M and Cucinella S 1987 *The Chemistry of Inorganic Homo and Heterocycles* ed I Haiduc and D B Sowerby (New York: Academic) pp 167–90
[31] Fowler P W 1986 *Chem. Phys. Lett.* **131** 444
[32] Zhao M W, Xia Y Y, Liu X D, Tan Z Y, Huang B D, Song C and Mei L M 2006 *J. Phys. Chem.* B **110** 8764